

## Methanol Oxidation on Vanadium Oxide Catalyst Prepared by *in Situ* Activation of Amorphous Vanadium Pentoxide Precursor

DANIEL GASSER AND ALFONS BAIKER<sup>1</sup>

*Department of Industrial and Engineering Chemistry, Swiss Federal Institute of Technology,  
ETH—Zentrum, CH-8092 Zürich, Switzerland*

Received February 16, 1988; revised April 20, 1988

Amorphous vanadium pentoxide was prepared using the sol-gel process and vanadyl triisobutoxide as precursor. The catalytic properties of this material for methanol oxidation to formaldehyde were investigated in the temperature range 300 to 520 K. At 520 K the initial activity of the amorphous  $V_2O_5$  was very low. However, during *in situ* activation at this temperature the activity increased steadily and reached a steady-state value which was about 30 times higher than the initial activity of the amorphous  $V_2O_5$  and also considerably higher than the activity of crystalline  $V_2O_5$ . X-ray diffraction indicated that upon exposure to methanol oxidation conditions the amorphous vanadia crystallized slowly and was partly reduced. These changes were accompanied by drastic alterations of the bulk and surface structure of the amorphous precursor as evidenced by electron microscopy. The final catalyst exhibiting steady-state activity consisted of crystalline  $V_2O_5$  and  $V_3O_7$ . Partial reduction of the bulk was not observed with crystalline vanadia catalysts and appears to be characteristic for the amorphous vanadia. The results indicate that amorphous vanadia undergoes structural changes more easily than its crystalline counterpart and may thus be an interesting catalyst precursor. © 1988 Academic Press, Inc.

### INTRODUCTION

Vanadium pentoxide supported or unsupported is a well-known catalyst for various mild oxidation processes (1, 2). It has been shown that its activity and selectivity in a particular reaction may depend markedly on the grain morphology, i.e., on the distribution of the exposed crystal faces. In many studies of oxidation reactions on vanadium pentoxide (3–9), the active sites were considered to be the  $V^{5+}=O$  species located on the (010) face. Tatibouet and Germain (10) prepared by fusion and slow recrystallization monocrystalline grains of orthorhombic  $V_2O_5$ , exposing the (001), (100), and (010) faces, and studied the oxidation of methanol on these catalysts at 540 K. They observed three different products: formaldehyde, methylal, and dimethyl ether. The authors found, at very low conversions, a significant variation of the ac-

tivities and selectivities between samples of different morphology and concluded that the (001) face is exclusively responsible for the methylal formation. According to their study, the (100) and (010) faces do not exhibit such a clear selectivity, although the (010) face was suggested to favor formaldehyde and ether formation.

More recently, we have studied methanol oxidation on  $V_2O_5$  samples with largely different contributions of the (010) faces to the surface area (11). In these studies which were performed in a fixed-bed microreactor in the temperature range 500–650 K no significant effect of grain morphology on methanol conversion and selectivity to formaldehyde was observed. However, selectivity was found to be strongly correlated with conversion.

In order to gain further insight into the relation between the structure of vanadia and its behavior in methanol oxidation we have used a different strategy in this work. Methanol oxidation was studied over

<sup>1</sup> To whom all correspondence should be addressed.

amorphous vanadium pentoxide and its catalytic behavior was compared to that of crystalline  $V_2O_5$ .

## EXPERIMENTAL

### *Catalyst*

The amorphous vanadium pentoxide (sample A) was prepared using the sol-gel process (12) and vanadyl triisobutoxide as precursor. The vanadyl triisobutoxide was synthesized according to Ref. (13). The isobutanol formed was removed by evaporation under reduced pressure at 323 K and a dark red  $V_2O_5$  sol was obtained. Subsequently the sol was dried at 323 K for 24 h and at 393 K for 72 h. After drying the dark blue material was ground and the sieve fraction of 100- to 200- $\mu\text{m}$  grains was used in the experiment.

Two crystalline vanadium pentoxide samples of different grain morphologies were used as references. Sample B consisted of well-developed platelets with the large faces corresponding to (010) planes; sample C contained poorly defined agglomerates of needle-type grains. Scanning electron micrographs showing the grain morphologies of samples B and C, respectively, have been presented in an earlier report (see Ref. (11)). Sample B was prepared by heating ammonia metavanadate for 2 h at 973 K and subsequently cooling it in the oven. Sample C was commercially available  $V_2O_5$  supplied by Fluka AG, Switzerland. Catalysts with grain sizes between 100 and 200  $\mu\text{m}$  were used in the experiments.

### *Catalyst Characterization*

The samples were characterized using gas adsorption (BET), X-ray diffraction (XRD), thermal analysis (TG, DTA), temperature-programmed reduction (TPR), scanning electron microscopy (SEM) and high-resolution electron microscopy (HREM). BET surface areas of the samples were measured by krypton adsorption at 77 K. Calculations were based on a cross-sectional area of 19.5  $\text{\AA}^2$  for a krypton atom,

which is the mean value of the range (17–22  $\text{\AA}^2$ ) quoted in the literature (19). X-ray diffraction patterns were obtained using a Philips diffractometer and  $\text{CuK}\alpha$  radiation. Thermal analysis experiments were performed on a Mettler TA 2000 C thermo-analyzer using argon as carrier gas. The heating rate was 0.167 K/s. Temperature-programmed reduction measurements of the samples were performed using the apparatus described in Ref. (14). Conditions employed were the following: amount of sample, 50 mg; heating rate, 0.167 K/s; reducing gas mixture, 6% hydrogen in argon; total flow rate, 1.25  $\text{cm}^3$  (NTP)/s.

### *Methanol Oxidation*

Methanol oxidation was performed in an isothermal continuous flow fixed-bed reactor using air as an oxygen source. The experimental arrangement used and the analytical procedure have been described in detail in a previous report (11). The reactant gas mixture was obtained by saturation of the air stream with methanol, i.e., by passing air through a bubble column filled with methanol at 280 K. Experiments performed with the crystalline  $V_2O_5$  samples (B and C) were started by heating the catalyst under air flow at 683 K for 2 h. The amorphous sample A was pretreated at a lower temperature, 393 K, to avoid crystallization. The catalytic tests were carried out under the following conditions: feed rate of methanol, 9.8  $\mu\text{mol/s}$ ; feed rate of air, 183  $\mu\text{mol/s}$ ; total pressure, 105 kPa; amount of catalyst corresponding to 0.365  $\text{m}^2$  (based on BET surface areas measured after pretreatment). Conversion and selectivity were defined as

$$\text{Conversion } C = \frac{\text{moles ME reacted}}{\text{moles FA formed}}$$

$$\text{Selectivity } S$$

$$= \frac{\text{moles FA formed}}{\text{moles (FA + DME + CO + CO}_2\text{)}}, \quad \text{formed}$$

where ME is methanol, DME is dimethyl ether, and FA is formaldehyde.

## RESULTS

### *Structural and Textural Properties of Fresh Catalysts*

The amorphous structure of sample A was confirmed by X-ray diffraction. XRD patterns showed a broad intensity maxima confirming the lack of long-range ordering of the constituents in this sample. The transition of the amorphous sample to the crystalline state was recorded by differential thermal analysis (DTA) combined with thermogravimetry (TG). Before crystallization the sample lost a substantial amount of water. The loss of water started at about 350 K whereas the exothermic transition from the amorphous to the crystalline state started at about 570 K. The final crystalline state was confirmed by XRD. XRD analysis of the crystalline samples B and C indicated that they consisted of pure  $V_2O_5$ . However, the platelets (sample B) oriented themselves in the X-ray sample holder, resulting in a considerable change in the intensity, in particular of the reflection characteristic of perpendicular planes, i.e., (010), (101), and (400). The largest changes have been observed for the reflections (010) and (101). The intensity ratios  $f = I_{101}/I_{010}$  determined for these samples were as follows: sample B,  $f = 0.30$ ; sample C,  $f = 0.87$ . The value  $f = 0.87$  of sample C is in good agreement with  $f = 0.90$  calculated for a monocrystal (15) and observed for nonoriented samples.

The BET surface areas measured for the catalysts after pretreatment in air were as follows: sample A,  $0.50 \text{ m}^2/\text{g}$ ; sample B,  $0.26 \text{ m}^2/\text{g}$ ; and sample C,  $1.48 \text{ m}^2/\text{g}$ .

Figure 1A shows the surface morphology of the amorphous sample A as seen by SEM. Temperature-programmed reduction indicated that the reduction behavior of samples A, B, and C was significantly influenced by the structural differences. The reduction profiles of the crystalline  $V_2O_5$  samples (B and C) were reported in previ-

ous work (11). With the amorphous  $V_2O_5$  (A) the onset of reduction occurred at a 40 K lower temperature, i.e., at about 810 K. This indicated that the amorphous sample was more easily reducible than the crystalline samples. Vanadium pentoxide was in all three cases reduced to  $V_2O_3$  as evidenced by XRD and the integral hydrogen uptake measured during TPR.

### *Structural and Textural Changes of Amorphous Precursor during in Situ Activation*

Figure 2 shows the change in activity of the amorphous precursor during *in situ* activation at 520 K. Note that the activity increased steadily up to about 14 h on stream. The steady-state activity reached after this time on stream was about 30 times higher than the activity of the amorphous precursor. In order to follow the structural changes occurring during the activation process, the experiment was repeated and samples were taken from the reactor at different times (indicated by arrows in Fig. 2) and analyzed by XRD. The results of these XRD analyses are presented in Fig. 3. We note that the amorphous precursor A crystallized slowly and was also partially reduced. The final catalyst which exhibited steady-state activity was crystalline and contained  $V_3O_7$  (16) as well as  $V_2O_5$  (Fig. 3, profile 4).

The structural changes were accompanied by an increase in the BET surface area from  $0.50$  to  $4.05 \text{ m}^2/\text{g}$ . The changes of the surface morphology occurring due to the *in situ* activation are illustrated in Figs. 1A and 1B. High-resolution transmission electron microscopy combined with electron diffraction indicated that well-developed monocrystals of  $V_2O_5$  grew out of the bulk material during the *in situ* activation. Figure 4 depicts the high-resolution electron micrograph of such a monocrystal together with the corresponding electron diffraction patterns.

In contrast to the amorphous sample A, the crystalline samples B and C only ex-

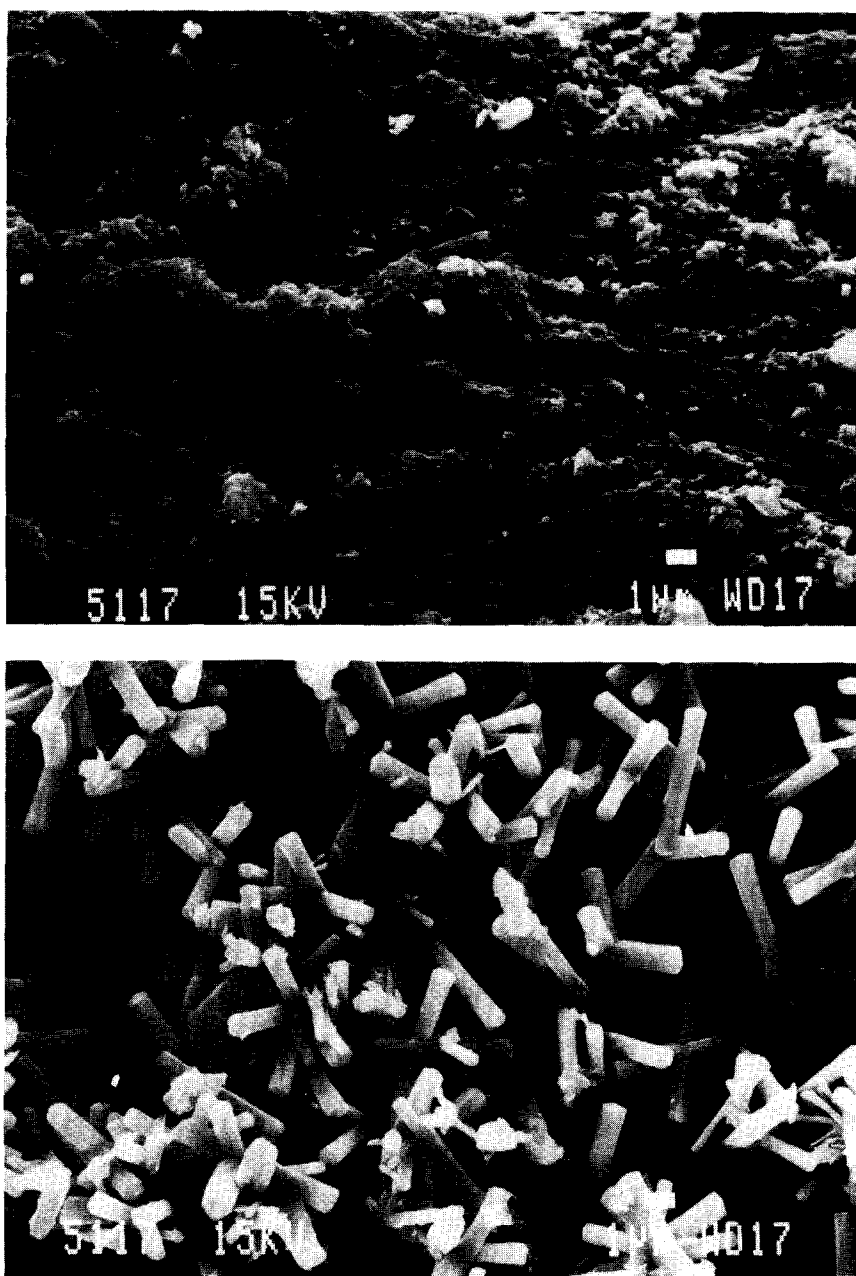


FIG. 1. Scanning electron micrographs showing the surface morphology of amorphous  $V_2O_5$  before (A) and after (B) *in situ* activation. Same magnification; the bar located at the bottom right side corresponds to  $1\ \mu\text{m}$ .

hibited a comparatively small increase in activity when exposed to reaction conditions for several hours. XRD analysis of the crystalline samples after reaction showed

the reflections of  $V_2O_5$  only; i.e., the bulk of the sample was not reduced under methanol oxidation conditions. Hence, the occurrence of a reduced vanadia phase  $V_3O_7$

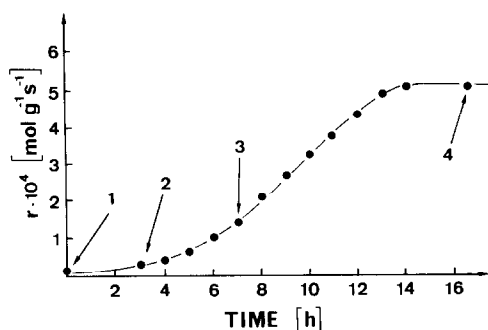


FIG. 2. Change of activity of the amorphous  $V_2O_5$  during *in situ* activation at 520 K. Methanol conversion rate is plotted versus time on stream. For conditions see under Experimental. Numbers indicate times when vanadia samples were taken from the reactor for analysis.

upon exposure to methanol oxidation was characteristic only for the amorphous sample A.

Finally, we should note that the crystalline samples also exhibited a marked increase in the BET surface area after several hours on stream. With sample B the BET surface area increased from 0.26 to 0.49  $m^2/g$ , and with sample C, from 1.48 to 2.9  $m^2/g$ . This increase in the surface area was caused by roughening of the surface as evidenced by SEM.

#### Catalytic Properties in Methanol Oxidation

Preliminary tests with respect to possible influences on the activity and selectivity caused by interparticle and intraparticle mass and heat transfer limitations (17) confirmed that such limitations could be ruled out under the conditions used in the catalytic tests. All experimental results reported were measured under steady-state conditions. Figure 5 compares the methanol conversion and the product distributions measured for the three vanadia samples.

The most important results emerging from Fig. 5 are as follows: (i) the catalyst prepared from the amorphous precursor

was considerably more active than the crystalline catalysts; (ii) with all catalysts the formation of dimethyl ether was significant at lower conversion, i.e., lower temperature, whereas at higher temperature the formation of CO and to a lesser degree of  $CO_2$  became relevant. Note the remarkable coincidence of the conversion and selectivity of the crystalline samples with different grain morphologies (samples B and C).

Specific rates for the formation of formaldehyde are compared in Fig. 6. Average rates  $r$  ( $mol/m^2 s$ ) were calculated from differential reactor experiments using the relation  $r = F/S$ , where  $F$  is the molar flow rate of formaldehyde leaving the reactor, and  $S$  the total catalyst surface area in the reactor. The apparent activation energies calculated from these data were as follows: sample A,  $84 \pm 3$  kJ/mol; sample B,  $95 \pm 2$  kJ/mol; and sample C,  $93 \pm 2$  kJ/mol.

#### DISCUSSION

The sol-gel process (12) consisting of hydrolysis and polycondensation proved to be a suitable method for the preparation of amorphous  $V_2O_5$  from a vanadyl alkoxide precursor. X-ray analysis did not give any indication of the presence of a crystalline phase in the fresh  $V_2O_5$  sample as prepared.

Aldebert *et al.* (18) proposed that  $V_2O_5$  gels consist of flat fibers cross-linked into layers. The fibers do not exhibit any orientation in the layer, but the distance of the layers is well-defined and depends on the water content of the gel. Our DTA and TG measurements showed that upon heating the gel loses water in two discernible steps. Crystallization occurred after the more strongly held water desorbed at about 460 K. This indicates that water stabilizes the amorphous gel structure. It appears that upon removal of the chemisorbed water the  $V_2O_5$  platelets are allowed to rearrange thereby allowing crystallization to occur.

As to the dependence of the activity of  $V_2O_5$  on its structural properties, the results shown in Fig. 2 indicate that the intrinsic

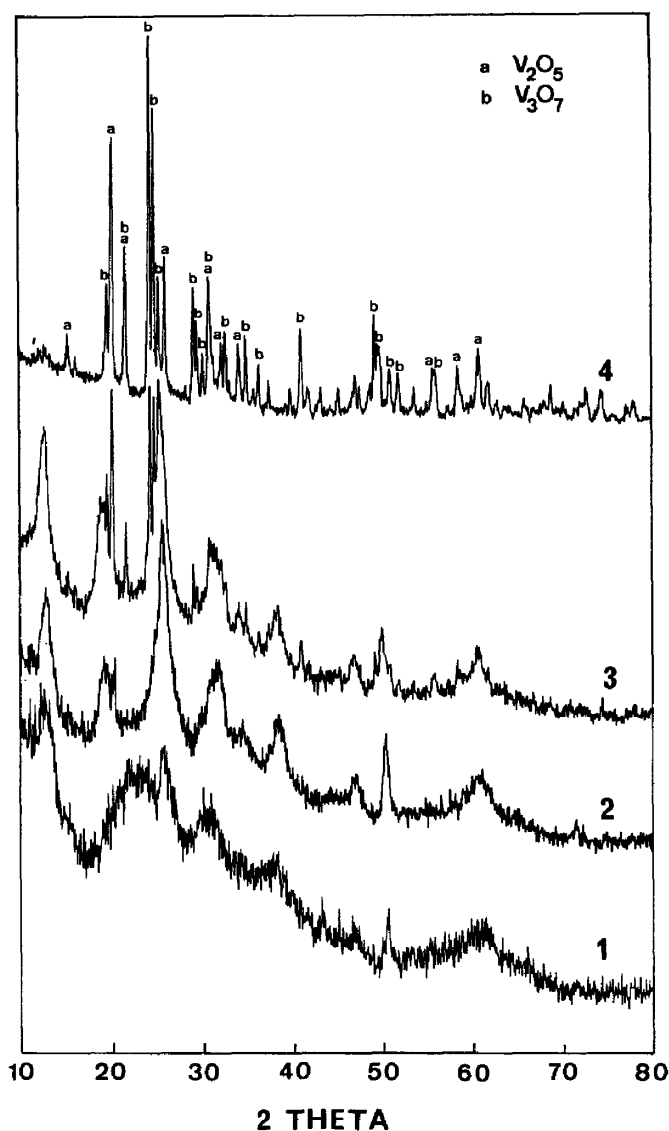


FIG. 3. Bulk structural changes which occurred during *in situ* activation of amorphous  $V_2O_5$  precursor analyzed by XRD. The numbers indicate samples taken after differing times from the reactor during the *in situ* activation experiment (see Fig. 2).

activity of amorphous  $V_2O_5$  for methanol oxidation is low compared to crystalline  $V_2O_5$ . The activity develops when the amorphous material starts to crystallize and the reduced phase ( $V_3O_7$ ) is formed. Thus two factors seem to be important for the activity, namely, the structure and the presence of a partially reduced phase. The influence of the structure on the activity

can be estimated roughly by comparing the formaldehyde formation rate  $r = F/S$  of the vanadia samples A, B, and C. At 520 K, the amorphous precursor exhibits an initial rate of about  $2 \times 10^{-5} \text{ mol/m}^2 \text{ s}$  (Fig. 2) compared to about  $3.5 \times 10^{-5}$  and  $4.5 \times 10^{-5} \text{ mol/m}^2 \text{ s}$  (Fig. 6) for the crystalline samples B and C, respectively. In the light of the dramatic structural changes occurring

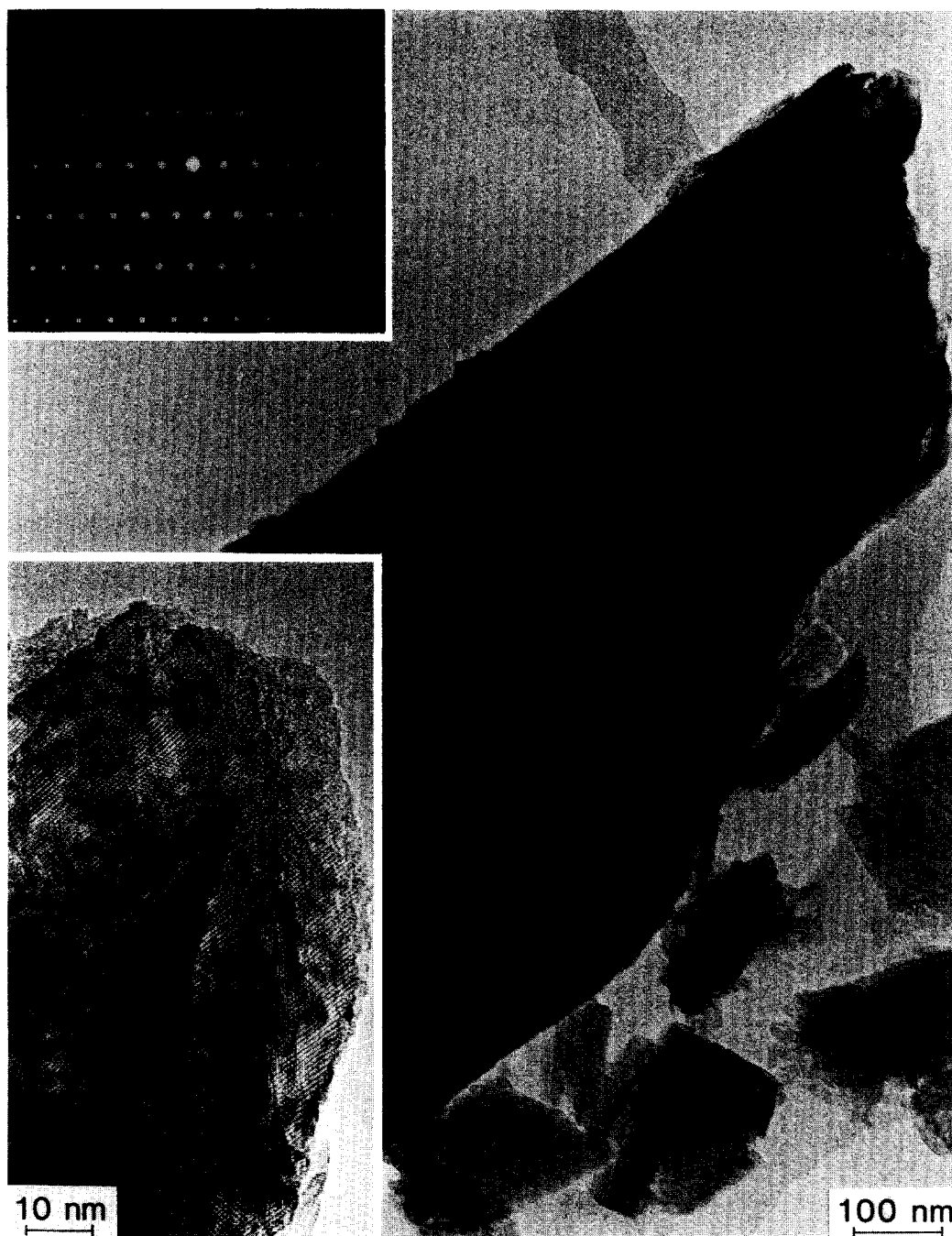


FIG. 4. High-resolution electron micrographs and electron diffraction pattern of the well-developed monocrystals of  $V_2O_5$  growing from the bulk structure of the amorphous precursor A during *in situ* activation at 520 K. Compare with scanning electron micrograph shown in Fig. 1B.

when going from the amorphous to the crystalline state, the difference in the activities seems to be rather small, indicating

only a weak structure sensitivity. The weak structure sensitivity is further supported by the similarity of the catalytic behavior of

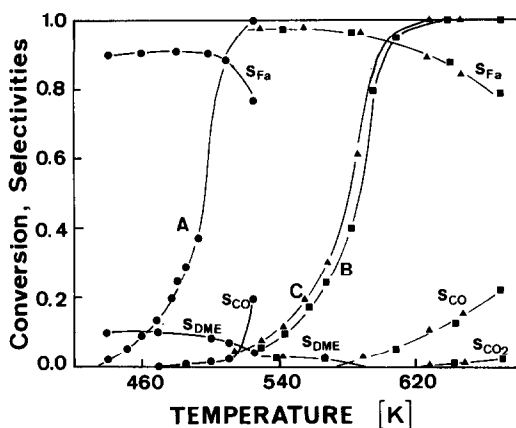


FIG. 5. Comparison of activity and selectivity of  $V_2O_5$  catalysts A (●), B (■), and C (▲) in methanol oxidation. Methanol conversion curves of the sample are also denoted by A, B, and C: Corresponding selectivities are designated by  $S_{FA}$ ,  $S_{DME}$ ,  $S_{CO}$ , and  $S_{CO_2}$ , where Fa represents formaldehyde and DME, dimethyl ether. Conditions: feed rate of methanol,  $9.8 \mu\text{mol/s}$ ; feed rate of air,  $183 \mu\text{mol/s}$ ; total pressure, 105 kPa; amount of catalyst corresponding to  $0.365 \text{ m}^2$  (based on BET surface areas measured after pre-treatment).

the two crystalline  $V_2O_5$  samples of different grain morphologies (see Figs. 5 and 6).

Hence, concerning the importance of the grain morphology of the crystalline  $V_2O_5$  with regard to its catalytic behavior in methanol oxidation we arrive at the same conclusions as are drawn in our previous study (11). Although possibly important at very low conversions, it appears that at higher conversions structural differences of the crystalline  $V_2O_5$  do not play a crucial role in activity and selectivity behavior. However, the selectivity appears to be strongly correlated with the methanol conversion. This may explain the difference between the results emerging from our studies and those of Tatibouet and Germain (10) who studied methanol oxidation at very low conversions. In contrast to their results we did not observe the formation of methylal and the product distribution only weakly depended on the grain morphology of  $V_2O_5$ .

Our results indicate that the activity of  $V_2O_5$  is markedly more influenced by the

presence of partially reduced vanadia species than by the bulk structural properties of the vanadium oxide. This emerges from a comparison of the steady-state activities (Fig. 6) at 520 K of catalyst A ( $1.3 \times 10^{-4} \text{ mol/m}^2 \text{ s}$ ) with those of catalysts B and C quoted above. Note that the activity of catalyst A which contained  $V_3O_7$  in addition to  $V_2O_5$  was about three to four times higher. It seems important to stress that the formation of a partially reduced vanadia phase ( $V_3O_7$ ) under methanol oxidation conditions was observed only with the amorphous  $V_2O_5$  precursor. Thus it appears to be characteristic for amorphous vanadia only.

Our studies indicate that amorphous vanadium pentoxide constitutes an interesting precursor for the preparation of vanadia catalysts, since it undergoes structural and

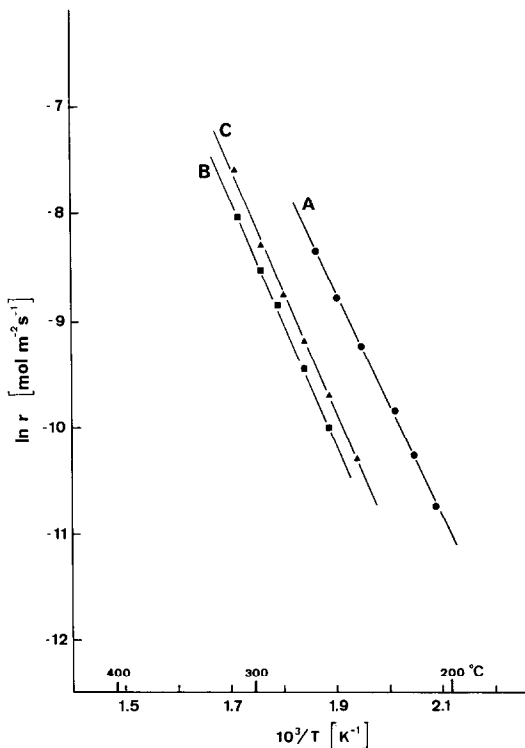


FIG. 6. Arrhenius plots of methanol oxidation rates measured over vanadia catalysts derived from amorphous precursor (A) and crystalline samples (B) and (C). For conditions see Fig. 5.

chemical changes more easily than the crystalline vanadia. Even *in situ* activation, i.e., exposure to reaction conditions, may suffice to prepare catalyst with markedly higher activities than exhibited by classically prepared crystalline vanadia.

### CONCLUSIONS

Methanol oxidation over crystalline vanadium pentoxide was found to be only weakly influenced by the grain morphology of the vanadia. This result emerged from a comparative study of methanol oxidation over vanadium pentoxides of different grain morphologies, i.e., vanadia with different contributions of the exposed faces to the surface. The selectivity of formaldehyde, dimethyl ether, and deep oxidation products (CO, CO<sub>2</sub>, H<sub>2</sub>O) was strongly dependent on the degree of methanol conversion.

Amorphous vanadium pentoxide exhibited only very low activity when exposed to methanol oxidation conditions at 520 K. However, the activity increased steadily with time on stream and reached finally a steady-state value which was more than an order of magnitude higher than the initial value and also considerably higher than the activity of the crystalline vanadia. X-ray diffraction and electron microscopy revealed that the amorphous vanadia crystallized slowly and was partly reduced to V<sub>3</sub>O<sub>7</sub> upon exposure to methanol oxidation conditions.

The presence of reduced vanadia species in the final catalyst seems to be an important factor explaining the high activity of the vanadia catalyst derived from the amorphous precursor. The presence of reduced phases after reaction was not observed with the crystalline vanadia samples which indicates that amorphous vanadia undergoes reduction more easily.

### ACKNOWLEDGMENTS

Thanks are due to Dr. A. Reller (University of Zürich) for the HREM and to P. Wägli (ETH-Zürich) for the SEM investigations. Financial support of this work by the Swiss National Science Foundation and the Board of the Swiss Federal Institutes of Technology and LONZA AG, Switzerland, is kindly acknowledged.

### REFERENCES

1. Volta, J. C., and Portefaix, J. L., *Appl. Catal.* **18**, 1 (1985).
2. Wainwright, M. S., *Catal. Rev. Sci. Eng.* **19**, 211 (1979).
3. Tamara, K., Yoshida, S., Ishida, S., and Kakioka, H., *Bull. Soc. Chem. Japan* **41**, 2840 (1968).
4. Kera, Y., and Hirota, K., *J. Phys. Chem.* **73**, 3973 (1969).
5. Nakamura, M., Kawai, K., and Fujiwara, Y., *J. Catal.* **34**, 345 (1974).
6. Cole, D. J., Cullis, C. F., and Hucknall, D. J., *J. Chem. Soc. Faraday Trans. 1* **72**, 2185 (1976).
7. Akimoto, N., Usami, M., and Echigoya, E., *Bull. Chem. Soc. Japan* **51**, 2195 (1978).
8. Gasior, M., and Machej, T., *J. Catal.* **83**, 472 (1983).
9. Baiker, A., Dollenmeier, P., He, R., and Wokaun, A., *J. Catal.* **100**, 345 (1986).
10. Tatibouet, J. M., and Germain, J. E., *C. R. Acad. Sci. Paris* **296**, 613 (1983).
11. Baiker, A., and Monti, D., *J. Catal.* **91**, 361 (1985).
12. Dislich, H., and Hinz, P., *J. Non-cryst. Solids* **48**, 11 (1982).
13. Funk, H., Weiss, W., and Zeising, M., *Z. Anorg. Allg. Chem.* **29**, 36 (1958).
14. Monti, D., and Baiker, A., *J. Catal.* **83**, 323 (1983).
15. ASTM Powder Diffraction File 9-387, Ed. Joint Committee on Powder Diffraction Standards, Pennsylvania, 1979.
16. ASTM Powder Diffraction File 27-940, Ed. Joint Committee on Powder Diffraction Standards, Pennsylvania, 1979; Walterson, K., Forsland, B., and Wilhelmi, K. A., *Acta Crystallogr. B* **30**, 2644 (1974).
17. Anderson, J. R., and Pratt, K. C., "Introduction to Characterization and Testing of Catalysts," p. 268 ff. Academic Press, London/San Diego, 1985.
18. Aldebert, P., Baffier, N., Gharbi, N., and Livage, J., *Mater. Res. Bull.* **16**, 669 (1981).
19. Gregg, S. J., and Sing, K. S. W., *Surf. Colloid Sci.* **9**, 254 (1976).